Chinese Journal of
POLYMER SCIENCE

RESEARCH ARTICLE

https://doi.org/10.1007/s10118-026-3720-8
Chinese J. Polym. Sci. **2026**, *44*, 3340–3354

From Waste to Coatings: Acidolysis of Polyurethane Elastomers with Itaconic Acid for Polyurethane Coating

Devesh Sane, Neel Godbole, Debarati Maity, and Anagha Sabnis*

Department of Polymer & Surface Engineering, Institute of Chemical Technology Nathalal Parekh Marg, Matunga (E), Mumbai-400019, India

Abstract This study explored the chemical recycling of polyurethane (PU) elastomers *via* acidolysis using itaconic acid and dimethylformamide (DMF) as the solvent without the use of glycol. The depolymerization process was optimized by varying the reaction parameters, and the resulting oligomers were analyzed using end-group analysis. PU coatings were formulated using recovered oligomers and isocyanates derived from isophorone diisocyanate (IPDI), hexamethylene diisocyanate (HDI), and toluene diisocyanate (TDI). Analytical techniques including differential scanning calorimetry (DSC), thermogravimetric analysis (TGA), Fourier-transform infrared spectroscopy (FTIR), electrochemical impedance spectroscopy (EIS), and gel permeation chromatography (GPC) were used for characterization. TDI based coatings exhibited superior optical, mechanical, chemical, thermal, and anticorrosive performance over the HDI and IPDIbased coatings. This study successfully showcased a facile method for recycling of PU waste along with PU coating formulations from 100% recycled oligomers, showcasing the use of recycled polyols in high performance applications.

Keywords Polyurethane; Acidolysis; Itaconic acid; Polyurethane coatings; Depolymerization

Citation: Sane, D.; Godbole, N.; Maity, D.; Sabnis, A. From waste to coatings: acidolysis of polyurethane elastomers with itaconic acid for polyurethane coating. *Chinese J. Polym. Sci.* **2026**, *44*, 3340–3354.

INTRODUCTION

As humanity has advanced and achieved higher living standards, the production and consumption of polymers has significantly increased. Polyurethane (PU) is one of the most versatile polymers and is used in many applications such as insulation materials, cushions and shoes for advanced applications in medical devices and aerospace components. Polyurethane is distinguished by the presence of multiple urethane linkages (—NH—C(=O)—O—) within its backbone regardless of the specific structural characteristics of the remaining polymer chain. PU synthesis primarily proceeds *via* condensation reactions between isocyanates and various polyols and may incorporate other functional groups, such as allophanates, esters, biurets, amides and ethers.[1–3]

Global PU production reached approximately 18 million metric tons in 2016, positioning it as the sixth most widely manufactured polymer, with a market valuation expected to surpass USD 81.7 billion by 2028.[4] However, the thermoset nature of most PU materials, combined with a diversity of formulations and additives, renders them inherently resistant to biodegradation and recycling, which necessitates proper management and disposal strategies.[5] As a result, a significant fraction of PU waste accumulates in landfills or is incinerated, releasing toxic gases such as hydrogen cyanide and nitrogen oxides.[6]

Although mechanical recycling has been deployed at a small scale, it often results in poor quality recyclates owing to the cross-linked architecture of thermoset PU's.[7,8] Thermochemical recycling approaches such as pyrolysis, gasification, and combustion convert polyurethane waste into energy, syngas or low-molecular-weight hydrocarbons through high-temperature processes.[9,10] These methods are particularly attractive for handling highly crosslinked or contaminated PU materials that are otherwise non-recyclable. While these recycling methods are sometimes considered the last resort in waste management hierarchies, they contradict the principles of the circular economy by converting polymeric materials into non-recoverable forms. In contrast, chemical recycling offers the advantages of functional group retention, lower carbon emissions and the possibility of reintegrating depolymerized products into high-value material streams, such as coatings, foams, and elastomers. As a result, chemical recycling has gained prominence as a sustainable strategy for PU waste valorization. Techniques, such as glycolysis, hydrolysis, aminolysis, and phosphorolysis, enable the breakdown of PU chains into reusable polyols or monomers. However, each approach presents specific drawbacks, such as high-energy input toxic byproducts (aromatic amines) and complex purification challenges.[11–16]

Acidolysis, a method involving the cleavage of urethane bonds using organic or inorganic acids, is increasingly being recognized as a promising chemical depolymerization route.

* Corresponding author, E-mail: as.sabnis@ictmumbai.edu.in
Received February 23, 2026; Accepted April 19, 2026; Published online July 1, 2026

First introduced in the 1980s, acidolysis has re-emerged as a viable alternative because of its ability to yield polyols without generating carcinogenic aromatic amines such as toluene diamine (TDA) or methylene diamine (MDA)[17,18] making it particularly attractive as an environmentally responsible recycling method.

Notably, a research group at the University of Aveiro (Portugal) made significant contributions to this area, identifying succinic acid as the most effective reagent for the acidolysis process.[19] At the laboratory scale, this research group successfully produced rigid polyurethane foams using up to 30% recycled polyol.[20] Gama *et al*. proposed a depolymerization scheme for acidolysis using succinic acid and phthalic acid as cleavage agents in a petroleum-based polyol medium. They identified the most likely chemical species present in the acidolysis product using NMR analysis.[21] Grdadolnik *et al*. investigated the microwave-assisted acidolysis of PU using adipic acid as the cleavage agent and a conventional polyol as the medium. The resulting product was pretreated with ethyl acetate to isolate monomeric compounds, which were then utilized in the production of flexible foam applications.[22] Omrani *et al*. utilized ricinoleic acid derivatives for the depolymerization of PU foams and were able to replace 30% of virgin polyol with the recycled ones in flexible foam applications.[23] Epps *et al*. reported a mild, phosgene-free method to depolymerize PUs into isocyanates using an organoboron Lewis acid at about 80 °C to depolymerize both thermoset and thermoplastic PUs into reusable isocyanates to synthesize new PUs. This approach promotes circularity and adds value to end-of-life PU products.[24] Baoyuan *et al*. reported a rapid, solvent free acidolysis process using maleic acid to depolymerize flexible PU foams, yielding 95% recycled polyol with properties comparable to virgin polyol in under 10 min. This method worked efficiently even with real mattress waste, demonstrating the practicality of this closed-loop recycling route. They also introduced a vapor-phase acidolysis approach using dicarboxylic acid at a temperature less than 150 °C, avoiding any byproduct formation and simplifying product purification. The process adhered to green chemistry principles and was successfully applied to post-consumer waste, making it practical, sustainable and energy-efficient.[25,26]

Itaconic acid offers several advantages over dicarboxylic acids explored to date. It has a higher dissociation constant (pK_{a_1}=3.84, pK_{a_2}=5.5), which can enhance the rate of urethane bond cleavage, whereas its shorter chain length promotes depolymerization efficiency[27] compared to other linear dicarboxylic acids, such as adipic acid (pK_{a_1}=4.41, pK_{a_2}=5.41) and succinic acid (pK_{a_1}=4.21, pK_{a_2}=5.64), exhibiting weaker acidity, and longer chain lengths reduce the reactivity and selectivity of the acidolysis reaction. Importantly, itaconic acid is derived from the fermentation of sugars by Aspergillus terreus, which aligns it with circular economy goals[28] and is also an inexpensive alternative to the dicarboxylic acids reported to date. Its high reactivity and environmental compatibility make it a compelling candidate for selective PU depolymerization. The use of itaconic acid with a polar aprotic solvent can eliminate the use of glycol[20–22,26–34] which tends to increase side reactions such as esterification, complexing the product composition, limiting the recyclate quality, and reducing the reaction temperature and time.

Recent studies have demonstrated the use of itaconic acid for the depolymerization of polyurethane flexible foam waste without using a catalyst or solvent, thus enabling the generation of functionalized products for 3D printing applications.[35] This approach primarily focuses on upcycling into a photocurable system and involves additional formulation steps. A comparison with previously reported acidolysis systems is shown in Table 1. This highlights that although several dicarboxylic acids have been explored, most systems require polyol media, catalysts, or additional purification steps.

This study explored the chemical recycling of PU elastomeric waste using itaconic acid as a cleavage agent in an aprotic solvent system (dimethylformamide, DMF) without using glycols or catalysts, enabling controlled depolymerization and direct utilization of the resulting oligomers for PU coating applications without any separation, purification, or blending with virgin polyols, demonstrating both simplicity and product utility.

MATERIALS AND METHODS

Materials

Pre-consumer PU elastomer waste was obtained from Jay Elastomers Pvt. Ltd. (Mumbai, India). Itaconic acid, xylene, dimethylformamide (DMF) and methyl ethyl ketone (MEK) were purchased from Oxford Lab Chemicals LLP (Mumbai, India). Desmodur-L75 (NCO content: 13.3%±0.4%, Non-Volatile Matter (NVM): 75±1), Desmodur-N75(NCO content: 16.5%±0.3%, NVM: 75±1) and Desmodur I (NCO content: ≥ 37.5%, NVM: 99.5±0.5) were provided by Covestro (India) Pvt. Ltd.

Depolymerization of PU Waste

The PU elastomer waste was manually cut into small pieces, approximately 5 mm × 5 mm in size, to facilitate uniform mixing and efficient depolymerization. The shredded material was charged into a four-necked round-bottom flask fitted with an overhead mechanical stirrer, reflux condenser, thermocouple and nitrogen inlet to maintain an inert atmosphere throughout the reaction. Depolymerization was carried out *via* acidolysis using itaconic acid as the depolymerizing agent, without the addition of any catalyst. PU waste and itaconic acid were weighed, while *N*,*N*-dimethylformamide (DMF) was used as a polar aprotic solvent in a 2:1 weight ratio (PU:DMF) to ensure good solubility of the acid, effective stirring, improved mass transfer between the solid PU and acid and uniform heat transfer. To evaluate the influence of key process variables, the PU waste-to-acid ratio (4:1, 5:1, 6:1), reaction time (120, 180, 240 min) and reaction temperature (145, 155, 165 °C) were varied. In each experiment, a single parameter was varied, while maintaining the other two constants. The oligomeric product obtained was a viscous, dark brown liquid that was used directly for coating formulations without any purification or separation of the solvent as a base in the formulation of polyurethane coatings. However, for chemical and instrumental characterization of the oligomeric product, DMF was removed by distillation to ensure accurate results.

Characterization of PU Waste

A comprehensive quantitative evaluation of the PU waste was

Table 1 Comparison of different acidolysis process using various carboxylic acids.

Cleavage agent	Medium	Temperature (°C)	Time (min)	Hydroxyl value (mg of KOH/g of sample)	Acid value (mg of KOH/g of sample)	Purification	Remarks	Ref.
Succinic acid	Polyol medium	about 195	300	51.3	3.7	No	Requires polyol medium; 20% replacement in rigid foams	[21]
Adipic acid	Polyol + microwave	about 210–230	30	55–60	3–7	Yes	Requires purification; 100% recycled polyol used	[22]
Ricinoleic acid derivatives	Polyol free	about 200	840	45–55	1–3	Not reported	50% replacement in flexible foams	[23]
Maleic acid	Polyol free	about 175	about 15 min	54.1	6.1	Yes	Fast reaction; tested on model substrates & end of life foam	[26]
Succinic acid	Polyol medium	195–205	60–300	150–230	5–12	No	30% replacement in rigid foams	[33]
Maleic acid + Phthalic acid	Polyether polyol+ H_2O_2	190–220	360–720	60–90	Not reported	Not reported	20% replacement in flexible foams	[34]
Succinic acid	Polyether polyol	205	180	35–50	1–6	Not reported	28% replacement in adhesives; Reaction conditions were optimized	[30]
Succinic acid	Polyether polyol + ZnAc catalyst	200	180	38–50	0–1	Not reported	40% replacement in flexible foams; Catalyst assisted system	[31]
Itaconic acid	Polyol free	about 180	about 60	Reactive hydrogen is mentioned, value is not reported	Reactive hydrogen is mentioned, value is not reported	Not reported	For 3D printing applications	[35]
Itaconic acid	Polar aprotic solvent (glycol-free)	about 165	about 180	140–150	25–30	No	Direct use, no purification, 100% utilization of recycled product	This work

performed using both proximate and ultimate analyses. In accordance with ASTM D3172, proximate analysis involves measuring the moisture content, volatile matter, ash content and fixed carbon content. The fixed carbon content was calculated using Eq. (1).

$$\text{Fixed carbon content (\%)} = 100 - (\text{moisture content} + \text{ash content} + \text{volatile matter percentage}) \quad (1)$$

Moisture content was determined according to the ASTM D3173 standard. A predetermined amount of the sample was subjected to drying in an oven at 105 °C for one hour. After drying, the samples were allowed to cool in a desiccator before being weighed again. This procedure was repeated until a constant sample weight was achieved. The moisture percentage was then calculated from the weight loss using Eq. (2).

$$\text{Moisture content (\%)} = \left[\frac{W_i - W_d}{W_i}\right] \times 100 \quad (2)$$

where W_i is initial weight of sample and W_d is sample weight after drying.

The volatile matter content of the waste was determined according to ASTM D3175. A pre weighted dried sample was placed in a lidded crucible and heated in a muffle furnace at 950 °C for seven minutes. After heating, the crucible was cooled in a desiccator and weighed. The percentage of volatile matter was calculated based on weight loss using Eq. (3).

$$\text{Volatile matter (\%)} = \left[\frac{W_d - W_s}{W_d}\right] \times 100 \quad (3)$$

where W_d is weight of dried sample and W_s is weight of remaining sample.

The ash content of the waste was analyzed according to ASTM D3174. The crucible containing the residue from the volatile matter test was heated in a muffle furnace at 700 °C. After cooling in a desiccator, the crucible was weighed and this process was repeated until a constant weight was obtained. The ash content was calculated based on the weight of the residue, using Eq. (4).

$$\text{Ash content (\%)} = \left[\frac{W_{cf} - W_c}{W_d}\right] \times 100 \quad (4)$$

where W_{cf} is weight of crucible and remaining ash after burning the sample at 700 °C, W_c is weight of crucible and W_d is sample weight after drying.

For the elemental composition analysis of the waste, UNICUBE Elementar Organic Elemental Analysis (Germany) was used. A precisely weighed sample was placed inside a tin capsule and subjected to combustion in a high-temperature furnace in a pure oxygen environment. The resulting combustion gases, including carbon dioxide, water vapor, nitrogen oxides and sulfur dioxide, were separated using a gas chromatography column and subsequently detected using a thermal conductivity detector. The software of the instrument was used to determine the weight percentages of carbon, hydrogen, nitrogen, sulfur and oxygen in the sample.

Characterization of Depolymerized Products

The acid value of the depolymerized product was evaluated according to the ASTM D1639 standard. Approximately 1 g of the sample was dissolved in a neutral methyl ethyl ketone-toluene solvent mixture, followed by titration with a 0.1N alcoholic KOH

solution, using phenolphthalein as an indicator. Due to the dark color of the product, the color change was difficult to observe; hence, wherever the color change was not visible, the pH of the mixture was analyzed to confirm the endpoint of the titration. The acid value was determined using Eq. (5).

$$\text{Acid value } \left(\frac{\text{mg KOH}}{\text{g}}\right) = \left(\frac{56.1 \times N \times R}{W}\right) \quad (5)$$

where N is normality of KOH, R is burette reading of sample and W is weight of sample.

The hydroxyl content was quantified according to the ASTM D1957 standard. Precisely weighed samples were subjected to reflux with an acetylation mixture (pyridine: acetic anhydride, 3/1, *V*/*V*) for 2.5 h, followed by addition of water. Water was introduced to hydrolyze any unreacted acetic anhydride followed by addition of 10 mL of *n*-butanol and the reaction mixture was titrated with 1N alcoholic KOH, using phenolphthalein as an indicator. The pH was evaluated in a manner similar to the acid value, where the color change was not visible. The hydroxyl value was calculated using Eq. (6).

$$\text{Hydroxyl value } \left(\frac{\text{mg KOH}}{\text{gm}}\right) = \frac{56.1 \times N \times (B - S)}{W} + \text{acid value} \quad (6)$$

where N is normality of KOH (N), B is volume of KOH solution (mL) required for blank, S is volume of KOH solution (mL) required for sample and W is sample weight (g).

The ester content was determined according to the ASTM D1617 standard. 1 g of sample was saponified by refluxing with 0.5N alcoholic KOH. Following saponification, the unreacted alkali was titrated with 0.5N aqueous HCl. The ester value was calculated using Eq. (7).

$$\text{Ester value } \left(\frac{\text{mg KOH}}{\text{g}}\right) = \left(\frac{56.1 \times N \times (B - S)}{W}\right) - \text{acid value} \quad (7)$$

where N is normality of HCl, B is volume of HCl solution (mL) required for blank, S is volume of HCl solution (mL) required for sample and W is sample weight (g).

Fourier transform infrared spectroscopy (FTIR) analysis was performed using a BRUKER ALPHA spectrophotometer with a spectral range of 4000–500 cm^{-1} and a resolution of 4 cm^{-1}. Gel permeation chromatography (GPC) was performed using a Perkin Elmer Turbo Matrix-40 analyzer connected to a refractive index detector to determine the number-average molecular weight and weight-average molecular weight of the depolymerized oligomeric product. The samples were dissolved in HPLC-grade tetrahydrofuran (THF) and injected into a column for analysis. Differential scanning calorimetry (DSC) was conducted on the waste and depolymerized oligomeric products in a nitrogen environment using a DSC Q-100 (TA instruments, USA) calibrated with n-octane and indium. The samples were analyzed in the temperature range of from −20 °C to 160 °C at a heating rate of 10 °C/min.

Coating Applications

The depolymerized oligomer was utilized as a base resin to formulate polyurethane coatings. Mild steel substrates (125 mm × 75 mm × 0.8 mm) were thoroughly cleaned by immersion in a degreasing solution for 15 min, followed by rinsing with water and wiping with cotton. Subsequently, the substrates were treated with acetone to remove any residual contaminants. The cleaned mild steel substrates were then dried in a hot air oven at 120 °C for 20 min and were further polished manually using an 80 grit emery paper.

PU coatings were formulated by reacting the oligomers obtained from batch E2 without further purification with three different isocyanates: Desmodur L-75 (toluene diisocyanate TDI-based), Desmodur N-75 (hexamethylene diisocyanate HDI-based) and Desmodur I (isophorone diisocyanate IPDI-based). The NCO index was maintained at a value of 1. A solvent mixture of *N*,*N*-dimethylformamide (DMF), xylene and methyl ethyl ketone (MEK) in a ratio of 5:3:2 (*W*:*W*:*W*) was used keeping the non-volatile matter (NVM) content at 40%. The amount of isocyanate required was calculated based on the hydroxyl equivalents of the depolymerized product, using Eq. (8).

$$\text{Amount of isocyanate} = \frac{\text{weight of recycled oligomer} \times \text{equivalent weight of isocyanate}}{\text{equivalent weight of recycled product}} \quad (8)$$

The formulated coatings were applied to prepared mild steel substrates using the flow method. After application, the coatings were allowed to flash off for 15 min, followed by curing at 120 °C for 20 min.

Because the oligomeric product was derived from waste with an undefined and variable structure, no standard formulation was used for direct one-to-one comparison with a conventional virgin polyol system. It is well established that the properties of PU coatings are highly dependent on the chemical structures of both the polyol and isocyanate, hydroxyl value, NCO index, molecular weight and curing conditions. Therefore, direct benchmarking against virgin polyol systems may not yield meaningful comparisons. Although literature reports provide a range of properties for PU coatings, these systems are often tailored for specific applications and compositions, making direct comparisons challenging. Instead, the present study focused on demonstrating the functional applicability of recycled oligomers across multiple performance parameters, including thermal stability, mechanical properties, chemical properties and corrosion resistance, thereby establishing their suitability for coating applications.

Characterization of Coatings

The mechanical, physical, chemical, optical and anticorrosive properties of the coatings were evaluated using standardized tests. The dry film thickness (DFT) was measured following IS 104 by calibrating the probe on an uncoated surface and averaging the readings from the different coated areas. Gloss at a 60° angle was determined according to ASTM D523 using a Rhopoint-Novagloss glossometer, with measurements taken from at least five locations on the coated steel panels for uniformity. The pencil hardness was assessed using ASTM D3363, employing a series of pencils from 6B to 6H, with the hardest pencil that did not scratch or cut the film being reported. Impact resistance was tested on coated mild steel panels following ASTM D2794 by dropping a 1.36 kg weight from 60 cm onto the coated surface to determine crack resistance. The direct impact on the coated surface was termed the "intrusion, and the indirect impact was referred to as "extrusion". Adhesion testing was conducted according to ASTM D3359 using a cross-cut test with commercially available adhesive tape to assess coating adherence based on a standard classification scale. Flexibility was

evaluated using a conical mandrel according to ASTM D522 by observing the coated aluminum panels for crack formation after bending. Coatings with no cracks are represented as zero "0" mm.

Chemical resistance was tested by immersing the coated panels in 1.25 mol/L aqueous sodium hydroxide and 1.37 mol/L aqueous hydrochloric acid for 24 h at ambient temperature, following ASTM D1308-2, with observations of blistering, discoloration and changes in gloss. The solvent resistance was tested using ASTM D4752-10, applying double rubs with xylene and methyl ethyl ketone up to a maximum of 200 rubs. Water absorption was measured according to ASTM D570-98 by immersing the pre-weighed coating samples in water for 24 h and calculating the weight difference. The water absorption was calculated using Eq. (9).

$$\text{Water absorption} = \frac{W_1 - W_0}{W_0} \times 100 \quad (9)$$

where W_0 and W_1 are the weights of the samples before and after immersion in water, respectively.

The hydrolytic stability of the films was assessed according to ASTM B1308 by immersing the films in boiling water for 4 h and evaluating the subsequent damage.

The extent of curing was determined by a solubility test using tetrahydrofuran (THF). The samples were then immersed in THF for 24 h, dried and weighed. The percentage of undissolved film was calculated to determine the extent of curing using Eq. (10).

$$\text{Extent of curing (\%)} = \frac{W_1}{W_0} \times 100 \quad (10)$$

where W_0 and W_1 are the weights of the cured films before and after immersion in THF, respectively.

The anticorrosion performance was assessed according to ASTM B117 by exposing the coated mild steel panels marked with crosswise scratches to a 5% NaCl salt spray at 35 °C for 500 h. Throughout this period, the coatings were monitored for signs of blistering, discoloration or loss of adhesion.

Electrochemical corrosion resistance was further assessed using a VersaSTAT-3 electrochemical workstation (AMETEK, Princeton Applied Research, USA) in a 3.5% NaCl solution at ambient temperature. A conventional three-electrode setup comprised a saturated calomel electrode (SCE) as the reference electrode, a platinum wire as the counter electrode and a coated mild steel panel as the working electrode. All the electrochemical measurements were conducted in triplicate, maintaining an exposed coating area of 21 cm^2 to ensure data reproducibility and consistency.

$$\text{Corrosion rate}\left(\frac{\text{mm}}{\text{year}}\right) = \frac{k \times I_{corr} \times EWs}{\rho s \times A} \quad (11)$$

where k is corrosion rate constant (3.27×10^{-3} mm·g/(μA·cm·year)), I_{corr} is corrosion current (A), EWs is equivalent weight of mild steel (28.25), ρs is density of mild steel (7.85 g/cm^3) and A is exposed surface area (1 cm^2).

For thermal analysis, differential scanning calorimetry (DSC) was performed on the cured coatings, as mentioned in the earlier section. Thermogravimetric analysis (TGA) of the cured films was performed on an SDT Q600 (TA Instruments) to study the thermal degradation properties. The analysis was carried out at a heating rate of 10 °C/min under nitrogen gas flow of 50 mL/min at temperatures ranging from room temperature to 650 °C.

RESULTS AND DISCUSSION

Proximate and Ultimate Analysis of Waste

Proximate analysis of the PU elastomer waste was performed to determine its basic compositional characteristics. The elastomer exhibited a high volatile matter content of 96.98%, with a relatively low fixed carbon content of 1.1%, indicating the organic and decomposable nature of the waste. A minimal amount of inorganic residue and absorbed water in the waste was confirmed by 1.33% of moisture content and 1.28% of ash content.

Ultimate analysis provided further insight into the elemental composition of the elastomer. The carbon content was the highest at 54.27%, whereas hydrogen, nitrogen and oxygen were 6.94%, 3.96% and 34.83%, respectively. Sulfur was not detected in the waste. These values confirm the organic polymeric nature of PU waste and its suitability for chemical depolymerization, as the high carbon and oxygen contents support the potential for cleavage and functional group formation during acidolysis with itaconic acid.

Depolymerization of PU Waste

The depolymerization of polyurethane (PU) elastomeric waste was systematically investigated, focusing on the effects of the ratios of different PU waste-to-acid ratios, time and temperature on the resulting acid, hydroxyl and ester values (Table 2). Among these parameters, the acid value is a critical indicator of the reaction progress, with a reduction in the acid value reflecting the cleavage of PU chains and the formation of hydroxyl-functional oligomers, as depicted in Fig. 1.

The depolymerization mechanism illustrated in Fig. 1 involves the acidolytic cleavage of urethane, urea, allophanate and biuret linkages through nucleophilic attack of the carboxylic acid group on the electrophilic carbonyl carbon of these linkages. In the case of urethane groups, protonation of the carbonyl oxygen by the acid enhances the electrophilicity of the carbonyl carbon, facilitating cleavage to give hydroxyl functional oligomers along with substituted amides or carbamate intermediates, accompanied by CO_2 evolution. Similarly, urea and biuret linkages undergo cleavage to generate amine and amide functionalities, which may further react with dicarboxylic acid to form secondary amide linkages.

Allophanate linkages can decompose to yield urethane and amide functionalities, or may directly produce amide-containing functionalities along with hydroxyl functional species and CO_2. In addition to primary depolymerization reactions, competing side reactions may also occur, depending on the reaction conditions. The hydroxyl groups generated during urethane cleavage can react with the carboxylic acid groups of itaconic acid to form ester linkages. Furthermore, amine groups formed from urea or biuret cleavage may react with dicarboxylic acids to form amide linkages.

In addition to these parameters, the role of the reaction medium was examined to understand its influence on depolymerization efficiency and reaction behavior. As a polar aprotic solvent, DMF facilitated the dissolution of itaconic acid and improved the mass transfer between the solid PU matrix and acid. In the absence of DMF, the reaction mixture

Table 2 Acidolysis of PU waste.

Batch No.	PU waste to acid (Weight basis)	Time (min)	Temperature (°C)	Acid value (mg of KOH/g of sample)	Hydroxyl value (mg of KOH/g of sample)	Ester value (mg of KOH/g of sample)
Varying PU waste to acid ratio						
E1	4:1	180	165	85	49	524
E2	5:1	180	165	34	156	440
E3	6:1	180	165	30	110	506
Varying reaction time						
E4	5:1	120	165	48	89	433
E5	5:1	180	165	27	120	489
E6	5:1	240	165	24	126	491
Varying reaction temperature						
E7	5:1	180	145	28	51	1674
E8	5:1	180	165	25	154	461
E9	5:1	180	185	20	99	548
Repeatability						
E10	5:1	180	165	28	149	476
E11	5:1	180	165	24	151	494

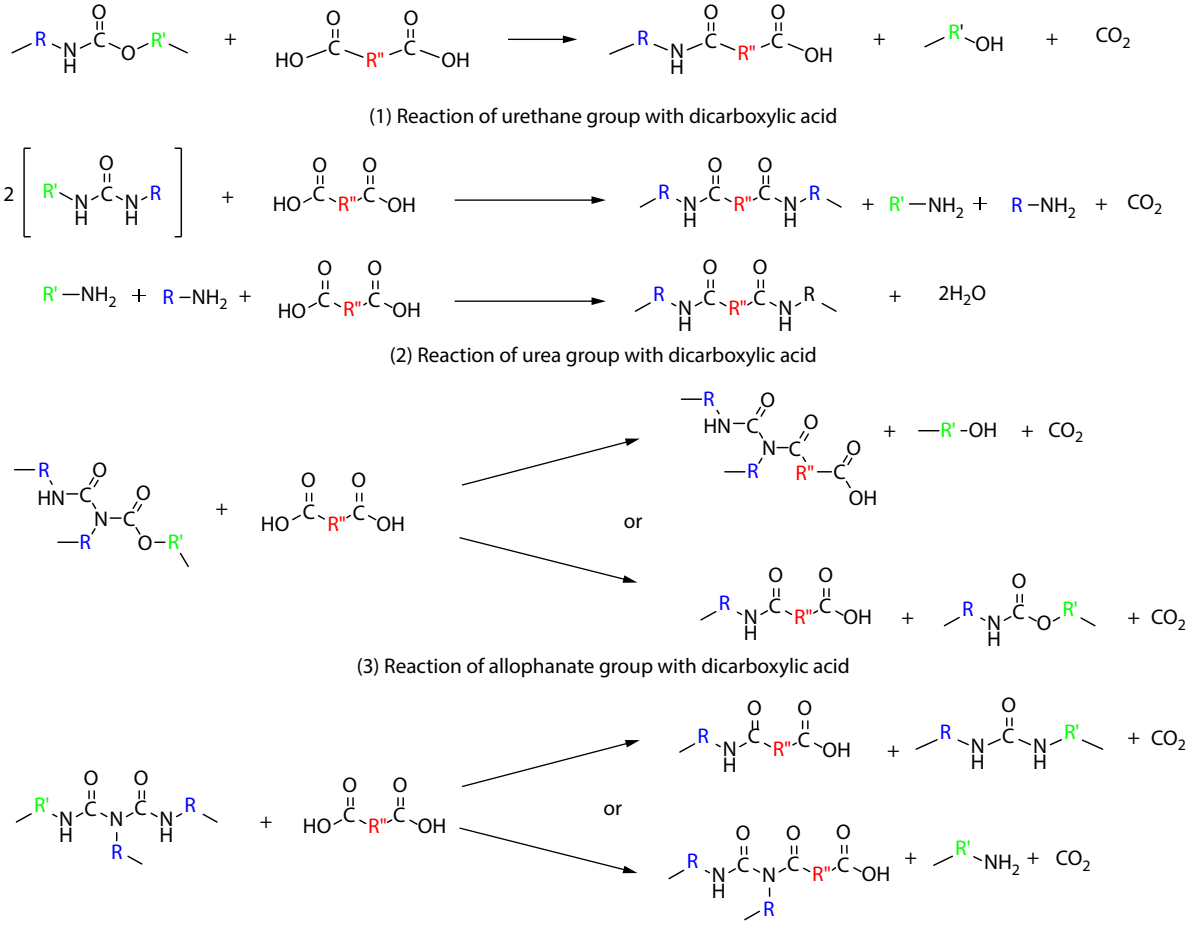

Fig. 1 Possible acidolysis reactions.

became highly viscous, leading to poor heat transfer and limited diffusion of acid species into the PU matrix, thereby slowing the depolymerization process. Thus, DMF enables more uniform reaction conditions and enhances reaction efficiency. Importantly, DMF did not participate in the acidolysis reaction and primarily acted as a physical medium. Compared to systems employing polyol as the reaction medium, the use of DMF avoids competing glycolysis reactions and minimizes esterification side reactions.

From a sustainability perspective, although DMF is a polar aprotic solvent with known toxicity concerns, its use in the present system offers certain practical advantages. The sol-

vent can be recovered *via* distillation during product characterization and in the present study it is directly utilized in subsequent coating formulations thereby eliminating the need for solvent removal as an additional step. This reduces the unit operation involved in decreasing process complexity.

The overall depolymerization efficiency was evaluated in terms of the product recovery. The reaction resulted in a high recovery of oligomeric product, with an overall yield of 87%–92%. Because the process did not involve any purification or separation steps, the entire depolymerized product was directly used in the coating formulations. Minor losses observed during the process can be attributed to the material adherence to the reactor surfaces, handling losses during charging, partial evaporation of DMF at elevated temperatures and the evolution of CO_2 (about 1.5%–2%) during acidolysis. The heterogeneous nature of PU waste and the absence of purification steps make precise mass-balance calculations challenging. However, the high overall recovery and direct utilization of the product indicate that the process is efficient and has potential for scalable applications.

Effect of the Ratio of PU Waste to Acid

A distinct trend emerged, as illustrated in Fig. 2, with respect to the ratio of PU waste to acid. As the ratio increased (*i.e.*, less acid was used relative to the PU waste), there was a significant decrease in the acid value from 85 mg KOH/g to 30 mg KOH/g (E1 to E3). This indicated that higher acid concentrations resulted in more residual acids in the mixture. Correspondingly, the hydroxyl value initially increased from 49 mg KOH/g to 156 mg KOH/g, suggesting an optimal ratio of 5:1 (PU waste: acid), after which it dropped to 110 mg KOH/g in E3. This could be due to the esterification reaction between the excess acid and hydroxyl groups. This trend was further confirmed by the ester values of 524 mg KOH/g (E1) to 440 mg KOH/g (E2). The ester value followed a nonlinear trend, with E2 exhibiting the lowest value (440 mg KOH/g), indicating a potentially better depolymerized intermediate for use as a polyol. This trend emphasizes the need for careful optimization of the acid concentration to balance the generation of hydroxyl groups and the formation of ester linkages, particularly if the goal is to maximize the polyol yield for further application.

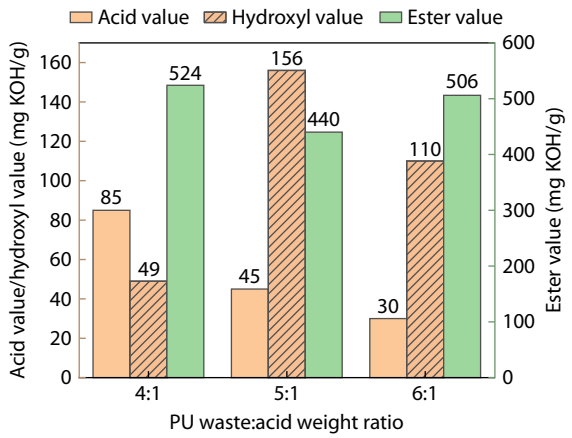

Fig. 2 Trend of acid, hydroxyl and ester values for different PU waste to acid ratios.

Effect of Reaction Time

With the 5:1 PU waste-to-acid ratio identified as optimal, the effect of the reaction time on this specific PU waste-to-acid ratio was subsequently examined as seen in Fig.3. In batch E4 (120 min), a relatively high acid value of 48 mg KOH/g was observed, which was undesirable because the residual acid in the product could negatively influence the final application of the depolymerized product. Extending the reaction time to 180 min (E5) significantly reduced the acid value to 27 mg KOH/g while maintaining a favorable hydroxyl value (120 mg KOH/g) and moderate ester content (489 mg KOH/g). However, carrying out the reaction for 240 min (E6) did not yield any substantial improvement, as the acid, hydroxyl and ester values remained nearly unchanged. This indicates that beyond 180 min, the reaction reaches a plateau and extending the reaction time offers no additional benefit while potentially consuming more energy and time.

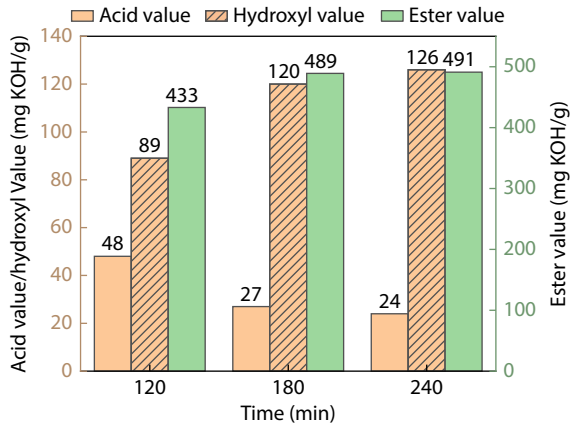

Fig. 3 Trend of acid, hydroxyl and ester values at different reaction time.

Effect of Reaction Temperature

Temperature was also observed to strongly influence the product characteristics as illustrated in Fig. 4. At 145 °C (E7), the hydroxyl value dropped drastically to 51 mg KOH/g and ester value increased to 1674 mg KOH/g, indicating extensive side reactions leading to ester formation. At 165 °C (E8), an optimal hy-

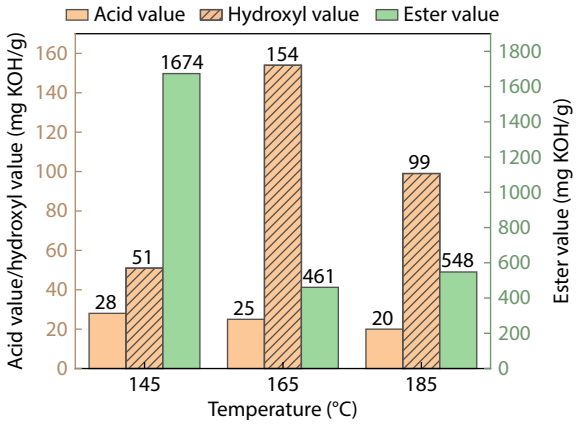

Fig. 4 Trend of acid, hydroxyl and ester values at different temperatures.

https://doi.org/10.1007/s10118-026-3720-8

droxyl value of 154 mg KOH/g and moderate ester value of 461 mg KOH/g were obtained, making it as the most effective reaction condition, a further increase to 185 °C (E9) led to decline in hydroxyl value to 99 mg KOH/g, likely due to thermal degradation or secondary reactions causing reduction in the availability of reactive hydroxyl groups.

Repeatability tests were conducted for the optimized reaction parameters (E10 and E11) and the results are listed in Table 3.

- PU waste-acid ratio = 5:1
- Reaction time = 3 h (180 min)
- Reaction temperature = 165 °C

Table 3 Repeatability of the batches under optimized conditions.

	Batch E10	Batch E11
Acid value (mg KOH/g)	28	24
Hydroxyl value (mg KOH/g)	149	151
Ester value (mg KOH/g)	476	494

Consistent results for the acid, hydroxyl and ester values for the optimized reaction parameters confirmed the reliability and reproducibility of the depolymerization process.

Kinetic Study: Effect of Temperature and Time on Functional End Groups

Initial experiments were conducted using waste-to-acid ratios of 4:1, 5:1 and 6:1, with measurements taken after 180 min. The 5:1 (PU waste: acid) ratio yielded the most favorable results, characterized by a low acid value, reduced ester formation and a satisfactory hydroxyl value. Based on these results, this ratio was chosen for a more detailed analysis to investigate the variations in acid, hydroxyl and ester values over time at different temperatures. The corresponding trends are illustrated in Figs. 5–7, highlighting the dynamic changes in these parameters throughout the reaction period. The study was conducted using the following variants:

- Time: 15, 30, 45, 60, 120, 180 min
- Temperature: 145, 155, 165 °C

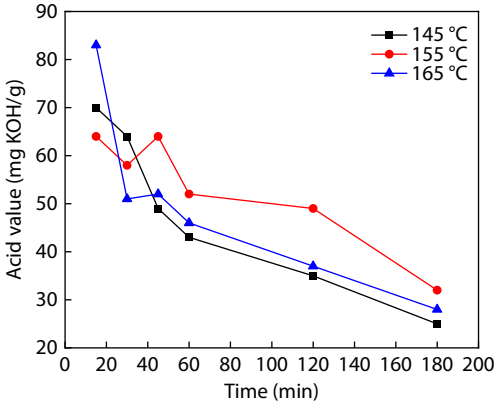

Fig. 5 Effect of temperature and time on acid value.

Effect of temperature and time on acid value

As illustrated in Fig. 5, the acid value consistently decreased with increasing reaction time across all three temperatures, indicating the reaction of free acid groups with urethane linkages to generate hydroxyl functionalities or due to the formation of ester linkages by the reaction of hydroxyl moieties with excess dicarboxylic acid.

At 145 °C the acid value dropped from 70 mg KOH/g at 15 min to 25 mg KOH/g at 180 min which is a 64% decrease. Similarly, a steady decline of 50% was observed at 155 °C (from 64 mg KOH/g to 32 mg KOH/g) and 66% at 165 °C suggested enhanced reaction kinetics at higher temperatures, facilitating more efficient acidolysis within shorter durations.

Effect of temperature and time on hydroxyl and ester value

The hydroxyl and ester values exhibit a more complex relationship with time and temperature, as illustrated in Figs. 6 and 7. At 165 °C the hydroxyl value initially decreases from 24 mg KOH/g (15 min) to 20 mg KOH/g (30 min), followed by a sharp increase to 113 mg KOH/g at 180 min. This initial trend, accompanied by an increase in ester value from 305 mg KOH/g to 376 mg KOH/g, may be due to early stage esterification of newly formed hydroxyl groups with excess carboxylic acid or ester linkages already present in the polymer backbone. However, as the reaction progressed, both hydroxyl and ester values increased sharply, indicating urethane cleavage and the reversal of ester linkages, regenerating hydroxyl and acid groups.

At 155 °C a similar pattern emerged. The hydroxyl value increased steadily from 64 mg KOH/g (15 min) to 149 mg (180 min), while the ester values also gradually increased from 383 mg KOH/g to 463 mg KOH/g. This simultaneous increase supports the hypothesis that urethane bond cleavage predomi-

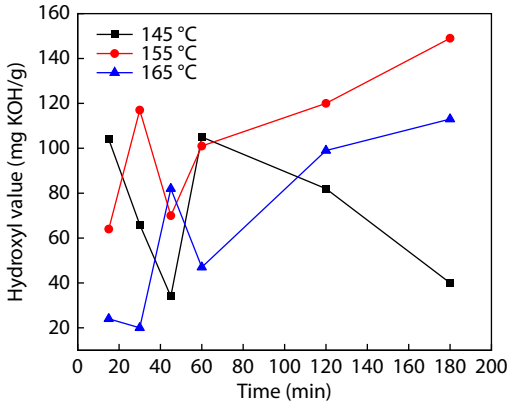

Fig. 6 Effect of temperature and time on hydroxyl value.

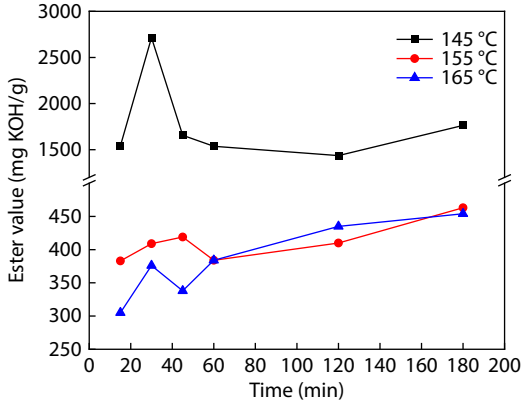

Fig. 7 Effect of temperature and time on ester value.

https://doi.org/10.1007/s10118-026-3720-8

nates over esterification and that partial hydrolysis of ester bonds may have occurred over prolonged durations.

At 145 °C, the hydroxyl value fluctuated and eventually declined at 180 min (40 mg KOH/g), while ester values remained exceptionally high throughout, peaking at 2715 mg KOH/g at 30 min and remaining above 1400 mg KOH/g at the end of the reaction. This high ester value can be attributed to the inherent ester functionalities present in the original PU backbone. At lower temperatures, incomplete depolymerization limited the cleavage of these ester segments, resulting in the continued presence of ester in the oligomeric product.

End group analysis revealed a clear relationship between the hydroxyl and ester values governed by depolymerization and side reactions. The initial decrease in hydroxyl values at the early stages is likely due to ester formation, while a subsequent increase may arise from both continued depolymerization and partial reversal of ester bonds. Among the three conditions, 165 °C for 180 min was optimal, achieving the highest hydroxyl value (113 mg KOH/g) with a moderate acid value (28 mg KOH/g) and considerable ester value (454 mg KOH/g), making it the most optimal condition for producing hydroxyl functional oligomers suitable for coating applications.

Spectroscopic Analysis

The PU elastomeric waste and oligomeric product (Batch E2) were analyzed using FTIR spectroscopy, as shown in Fig. 8. The broad transmission band at 3345 cm^{-1} in the elastomer waste was attributed to N—H stretching vibrations, indicative of urethane linkages. The band at 2952 cm^{-1} corresponds to aliphatic —CH_2 stretching vibrations, which are present in both samples with varying intensities. A marked decrease in the intensity of the band near 1534 cm^{-1} (N—H bending) in the recycled product further confirms the degradation of the urethane linkages. The C=O stretching at 1723 cm^{-1} corresponding to the ester linkages in the PU backbone shows an increase in intensity due to the formation of ester linkages, which is a result of side reactions between the acid and hydroxyl groups. Concurrently, a prominent peak at 1622 cm, corresponding to the C=O stretching of amide I, indicates the formation of amide bonds. Additionally, the appearance of a stronger band at 1379 cm (O—H bending) in the recycled product reflects the generation of hydroxyl-terminated oligomers. The increased intensity of the C—O stretching band at 1135 cm^{-1} in the recycled product indicates the presence of ether linkages or oligomers formed during acidolysis.

DSC Analysis of PU Elastomer and Depolymerized Product

The thermal behavior of the PU elastomer waste and recycled product (Batch E2) was investigated using differential scanning calorimetry (DSC), as illustrated in Fig. 9. The thermogram of elastomer waste, represented by a green curve, exhibited a distinct glass transition temperature (T_g) at –18.6 °C possibly due to the soft segments in the flexible polyurethane system. In contrast, the recycled product (red curve) did not exhibit a clear T_g within the scanned temperature range, indicating a significant alteration in its segmental structure. The absence of T_g suggests extensive chain scission during the depolymerization process, resulting in fragments with lower molecular weights. However, the recycled product curve displayed a broader and more pronounced deviation in the heat flow baseline beyond 50 °C, possibly because of the presence of lower molecular weight oligomers and unreacted acidic species.

Molecular Weight Analysis

The depolymerization of the PU waste was further confirmed by GPC analysis, as shown in Fig. 10. The number average molecular weight, weight average molecular weight and polydispersity index are tabulated in Table 4. M_n and M_w were observed to decrease with a reduction in the amount of the cleavage agent. In the case of E1, the excess dicarboxylic acid present in the sys-

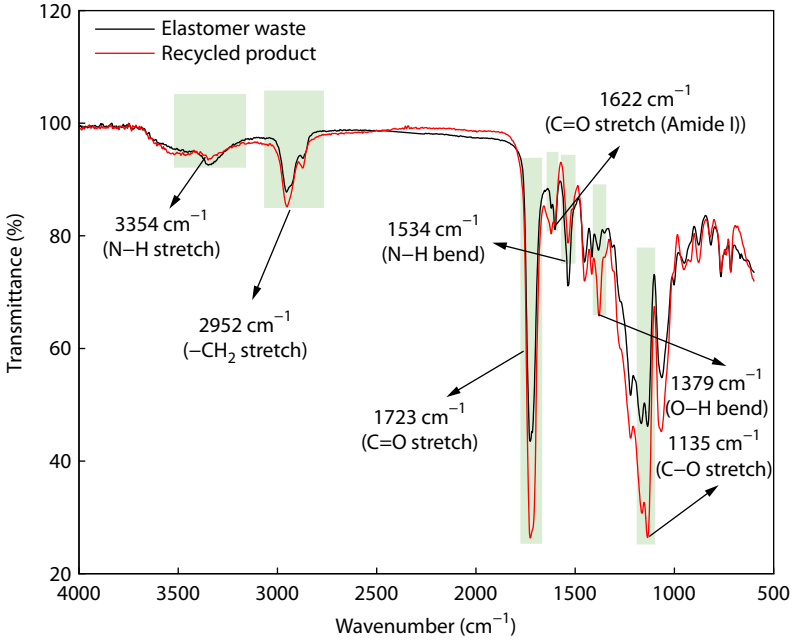

Fig. 8 FTIR spectra of PU waste and depolymerized product.

https://doi.org/10.1007/s10118-026-3720-8

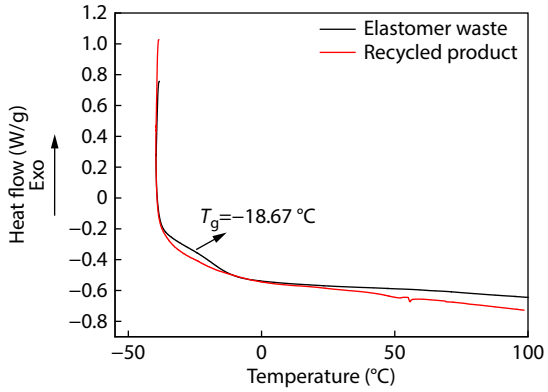

Fig. 9 DSC thermograms of PU waste and depolymerized product.

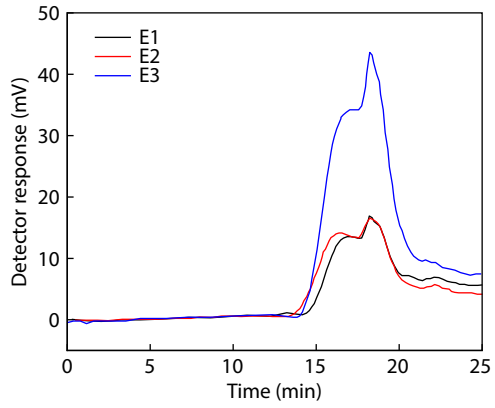

Fig. 10 GPC chromatograms of recycled oligomers.

Table 4 GPC chromatograms of recycled oligomers.

No.	Sample name	M_n	M_w	PDI
1	E1	696	1690	2.42
2	E2	385	451	1.17
3	E3	309	375	1.21

tem, as shown in Table 2, led to the formation of ester linkages, increasing the PDI as well as the molecular weight of the oligomers. In E2 and E3, there were very subtle differences in the polydispersity and molar mass ratio. This is likely because the lower amount of cleavage agent minimized secondary reactions, thereby restricting chain extension and yielding oligomers with comparatively shorter chain lengths.

General Coating Properties

Optical and mechanical properties

The optical and mechanical properties of the polyurethane coatings were evaluated through various tests and are summarized in Table 5. The high glossiness observed in the polyurethane coatings can be attributed to the inherent characteristics of the polyurethane backbone and crystallinity of the raw materials in the polymer matrix. Among the polyurethane coatings, the coatings prepared with toluene diisocyanate (TDI, Desmodur L-75) displayed a higher gloss than hexamethylene diisocyanate (HDI, Desmodur N-75) and isophorone diisocyanate (Desmodur I). This is likely due to the aromatic ring present in the TDI adduct, which facilitates ring flipping and the higher refractive index resulting from the significant molar refraction of aromatic groups owing to their large polarizability and high electron density. The IPDI-based coatings also exhibited good gloss, which could be attributed to the cycloaliphatic nature of the hardener. The cycloaliphatic configuration enhances the packaging efficiency, allowing more light to be refracted rather than diffused.

Adhesion properties were evaluated using a cross-cut adhesion test. All formulated coatings exhibited excellent adhesion to the metallic substrate, achieving a rating of 5B. This strong adhesion is likely due to the presence of polar linkages, such as urethane, which facilitates secondary bonding with the mild steel substrate.

Pencil and scratch hardness tests were conducted to measure the hardness of the coatings. The extent of curing and inherent structure of the polymeric backbone are the two major factors that contribute to hardness. The E2-TDI systems when compared to E2-HDI and E2-IPDI exhibited superior scratch hardness and comparable pencil hardness most likely due to the aromatic nature of the crosslinker which contributes to a denser, more rigid network. In contrast, the E2-HDI systems showed the lowest value, which could be attributed to the long flexible chains present in its backbone.

The impact resistance of any coating system depends on the ability of the coating to dissipate energy or the force of impact evenly throughout the film. All PU systems exhibited an excellent impact resistance of 70.86 lbs-in. These results can be attributed to the flexible, long chains present in the oligomeric depolymerized product, which confer significant free volume, allowing the coatings to absorb and distribute the impact energy effectively. Additionally, all coating systems demonstrated outstanding flexibility with no visible cracks after testing. The high flexibility is likely due to the strong adhesion between the substrate and the coated film, coupled with the presence of long flexible chains in the oligomeric product, irrespective of the hardener used.

Chemical properties

The chemical resistance of the coatings was evaluated by immersion tests in acidic (5% *W*/*W* HCl) and alkaline (5% *W*/*W* NaOH) solutions for 24 h, as shown in Table 6. All coatings demonstrated good resistance to both acids and alkalis; however, the coatings cured with hexamethylene diisocyanate (HDI) exhibited significant blistering, likely because of the high concentration of polar moieties, making them more susceptible to

Table 5 Optical & mechanical properties of PU coatings.

	DFT (μm)	Gloss (GU) @60°	Adhesion	Pencil hardness	Flexibility (mm)	Scratch hardness (gm)	Impact resistance (lbs.in)	
							Intrusion	Extrusion
E2-TDI	90-100	99	5B	4H	0	2000	70.86	70.86
E2-HDI	90-100	30	5B	3H	0	1600	70.86	70.86
E2-IPDI	90-100	63	5B	4H	0	1650	70.86	70.86

https://doi.org/10.1007/s10118-026-3720-8

Table 6 Chemical properties of PU coatings.

	Acid resistance	Alkali resistance	Hydrolytic stability	Solvent resistance	
				MEK	Xylene
E2-TDI	No change	No change	Whitish brown precipitation	>200	>200
E2-HDI	Black spots	No change	Rust spotting	186	>200
E2-IPDI	No change	Loss of adhesion	Rust spotting	195	>200

moisture and chemical ingress.

Rust spotting was evident on all PU coatings subjected to the hydrolytic stability test. This phenomenon can be attributed to the presence of polar linkages, which enable hydrogen bonding and facilitate moisture uptake. However, the absence of blistering suggests that the high extent of crosslinking and strong intermolecular hydrogen bonding among adjacent molecules helped prevent water penetration. The E2-TDI system displayed a whitish-brown precipitate, which may be attributed to hydrogen bonding between free hydroxyl groups and water or the reaction of residual isocyanate with water to form urea linkages.

The solvent resistance of the coatings was assessed using the double rubbing method with methyl ethyl ketone (MEK) as the polar solvent and xylene as the non polar solvent. All coatings exhibited excellent resistance to xylene with 200 double rubs, which can be attributed to the high extent of curing and the presence of polar moieties that resists non polar solvent attack. The TDI-based coatings demonstrated good MEK resistance despite the presence of polar groups, which is likely due to the tightly packed polymer network formed by ring stacking, resulting in less free volume, which inhibits the ingress of the solvent. However, the E2-HDI and E2-IPDI systems exhibited slight adhesion loss after 186 and 195 rubs respectively possibly because of the polar nature of MEK which facilitated the dissolution of polar moieties in the coatings.

Free film properties

The gel content of the cured films was measured to evaluate the extent of curing of the coating formulations. The cured films with known initial weights were immersed in tetrahydrofuran (THF) for 24 h, after which the weight loss of the dried films was recorded. The resulting extent of curing, which indicates the degree of network formation in the cured films, was observed to be in the range of 90% and 97%, as presented in Table 7.

Table 7 Free film properties of PU coatings.

	Gel content (%)	Water absorption (%)
E2-TDI	92	2.5
E2-HDI	97	1.3
E2-IPDI	90	1.0

Water absorption tests were conducted on the cured samples to assess the impact of the network structure on water uptake. Samples of known weights were immersed in water at room temperature for 24 h. Subsequently, excess water was removed by gently drying the samples with cotton and their weights were measured again. The water absorption was calculated based on the weight difference between the films before and after immersion. Among the formulations, E2-TDI coating exhibited higher water absorption than E2-HDI and E2-IPDI. This behavior can be attributed to differences in the network structure compared to the gel content alone. Owing to its trifunctional nature, the HDI-based system (Desmodur N-75) forms a more homogenous and densely packed network, thereby restricting water diffusion and resulting in lower water uptake. In contrast, the TDI-based system (Desmodur L-75), despite being trifunctional, contains aromatic isomers with differential reactivity, leading to a less uniform network structure with increased free volume and greater accessibility to polar urethane groups, which facilitates higher water absorption. The IPDI-based system, derived from a difunctional monomer, formed a comparatively less crosslinked network. However, its compact network structure limits the accessibility of polar groups, resulting in lower water uptake than that of TDI-based systems. It is important to note that the gel content reflects the extent of curing and the insoluble fraction of the network and does not directly represent the crosslink density. However, it provides a useful comparative indication of network formation across formulations.

Thermal Properties

Differential scanning calorimetry (DSC) thermograms of cured polyurethane coatings prepared from recycled polyol and different diisocyanates (TDI, HDI and IPDI) are shown in Fig. 11. The Glass transition temperatures (T_g) observed were 67.38 °C for E2-TDI, 59.69 °C for E2-IPDI and 53.09 °C for E2-HDI. The presence of a single T_g in each case indicated a reasonably homogeneous polymer network with no distinct microphase separation between the soft and hard segments. Among the three, the TDI-based coating exhibited the highest T_g, which may be attributed to the higher rigidity of its aromatic structure and relatively greater degree of phase restriction. In contrast, the aliphatic HDI-based coating exhibited the lowest T_g, suggesting more flexible chain segments and increased phase mixing.

No melting endotherms were observed in the DSC profiles of any sample. The absence of melting peaks confirms the

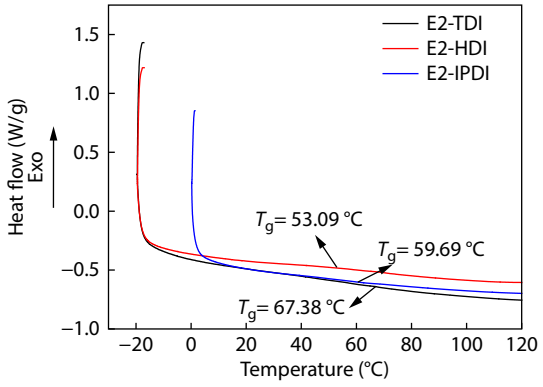

Fig. 11 DSC thermograms of PU coatings.

amorphous nature of the cured polyurethane networks and the highly crosslinked structure of the coatings. In such systems, the molecular mobility required for crystallization is significantly restricted and the material lacks sufficient regularity to form crystalline domains. Therefore, only glass transitions were evident and no sharp melting transitions were detected.

Thermogravimetric Analysis

The thermal stabilities of the polyurethane coatings derived from recycled polyols were evaluated by thermogravimetric analysis (TGA) and the results for the TDI, HDI and IPDI-based systems are presented in Fig. 12 and Table 8. All coatings exhibited a two-step degradation behavior, typical of polyurethanes, corresponding to urethane bond cleavage followed by degradation of the polyol backbone. Interestingly, the trend observed here deviates from the classical thermal stability order of the isocyanate systems (Aromatic > Cycloaliphatic > Aliphatic). The IPDI-based coating exhibited the highest degradation temperature, T_{10} = 282.7 °C and T_{50} = 366.6 °C but decomposed almost completely, leaving only about 4% char at 600 °C. In contrast, the HDI-based system showed the lowest 10% degradation temperature (T_{10}=243.3 °C) but retained the greatest char fraction (about 18%), while the TDI-based coating displayed intermediate stability with a char yield of about 11%.

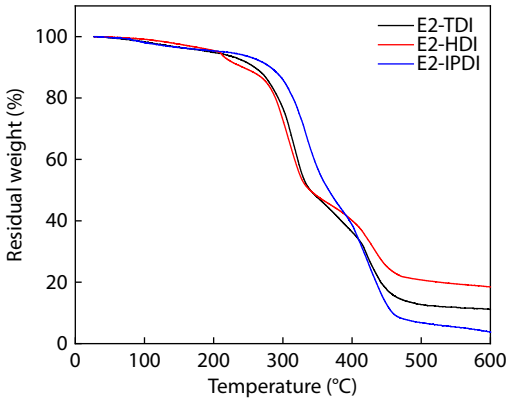

Fig. 12 TGA thermograms of PU coatings.

Table 8 TGA data of PU coatings.

Sample	T_{10} (°C)	T_{50} (°C)	T_{80} (°C)	Char yield (%)
E2-TDI	259.5	340.2	441.9	11.29
E2-HDI	243.3	339.7	528.8	18.56
E2-IPDI	282.7	366.6	459.2	3.94

Such deviations from theoretical expectations are consistent with literature reports that emphasize that the thermal degradation of polyurethane is controlled not only by the aromaticity of the isocyanate, but also by the crosslink density, functionality and polymer network.[36,37] In the present case, the gel content values align with the observed char yields (HDI 97% > TDI 92% > IPDI 90%), supporting the conclusion that high crosslink density promotes condensed phase stabilization during pyrolysis, thereby enhancing char formation. The superior performance of HDI-based coatings can be attributed to the use of Desmodur N-75, a trifunctional adduct that forms a highly homogenous and densely packed crosslinked network. The TDI-based system (Desmodur L-75) is also a trifunctional trimethylolpropane adduct, but its rigid aromatic segments and differential reactivity reduce the network uniformity, leading to a slightly lower char yield. In contrast, the IPDI coating (Desmodur I) is derived from a difunctional, sterically hindered monomer, which limits the crosslinking efficiency and explains its poor char yield despite the delayed onset of degradation. These findings are in agreement with earlier studies on the polyurethane degradation behavior, further validating the observed performance of the present coatings.

Tafel Analysis

Tafel polarization studies were conducted to evaluate the corrosion rate of polyurethane coatings derived from recycled products cured with TDI, HDI and IPDI-based isocyanates, as shown in Fig. 13. Key electrochemical parameters, such as the corrosion current density I_{corr} and corrosion potential E_{corr}, were derived from Tafel plots and the corresponding corrosion rates were calculated using Eq. (11) and are tabulated in Table 9. Among the three systems, the E2-TDI coating exhibited the lowest I_{corr} value of 1.01×10^{-8} A and the most negative E_{corr} at –0.705 V, indicating superior corrosion resistance amongst the series. This is further supported by the lowest corrosion rate of 1.18×10^{-4} mm/year. In comparison the E2-HDI and E2-IPDI coatings showed slightly higher I_{corr} values of 1.22×10^{-8} A and 1.10×10^{-8} A, respectively, with marginally increased corrosion rates. The enhanced performance of the TDI-based coating can be attributed to its aromatic structure, which promotes better barrier properties and tighter network packing owing to ring stacking, which limits the ingress of corrosive ions.[38] This is further explained in the next section of the frequency response analysis, which provides insights into the diffusion behavior and barrier properties of TDI-based systems.

Frequency Response Analysis

The Bode plot presented in Fig. 14 illustrates the impedance behavior of polyurethane coatings prepared from recycled oligomers cured with TDI, HDI and IPDI-based diisocyanates

Table 9 Corrosion rates of various coatings.

	I_{corr} (A)	E_{corr} (V)	Corrosion rate (mm/year)
E2-TDI	1.01×10^{-8}	–0.705	1.18×10^{-4}
E2-HDI	1.22×10^{-8}	–0.690	1.43×10^{-4}
E2-IPDI	1.10×10^{-8}	–0.666	1.29×10^{-4}

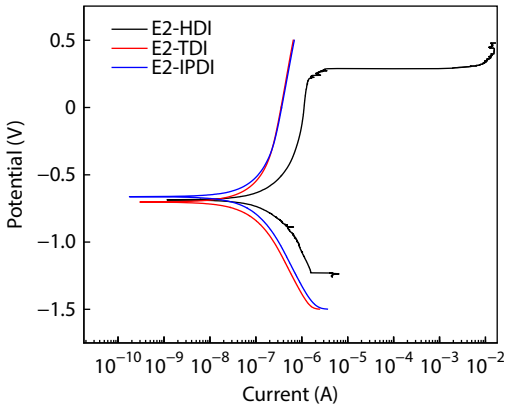

Fig. 13 Tafel analysis of polyurethane coating system.

https://doi.org/10.1007/s10118-026-3720-8

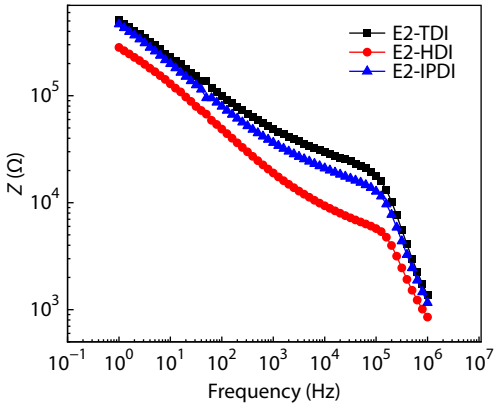

Fig. 14 Bode plots of polyurethane coating system.

over a frequency range and provides insights into the barrier properties and diffusion-controlled processes governing corrosion protection. The E2-TDI coating exhibited the highest impedance at the lowest frequency, indicating its superior barrier properties and resistance to electrolyte penetration through the coating matrix. This was followed by the E2-IPDI and E2-HDI systems, which displayed relatively low impedance values. The higher impedance observed for the TDI-based coating suggests the formation of a more tightly packed polymer network, likely due to the aromatic π-π stacking of TDI, which reduces the free volume, thereby preventing electrolyte ingress. In contrast, the E-2 HDI coating derived from aliphatic diisocyanate showed the lowest impedance, indicating a relatively lower resistance against corrosive species, potentially because of a more flexible network structure with greater segmental motion and higher free volume. The E2-IPDI coating displayed intermediate performance benefitting from its cycloaliphatic structure, which provided a balance between rigidity and flexibility, contributing to moderate crosslinking efficiency and barrier protection. These findings are in line with the Tafel polarization results and reinforce the fact that TDI-based coatings offer superior electrochemical protection in saline environments.

Anticorrosive Properties

The anticorrosive properties of the coatings were evaluated using a salt spray test according to ASTM B117. The coated panels were then exposed to 5 wt% of NaCl solution at 35 °C for a period of 500 h. Fig. 15 presents a visual comparison of the coatings at the start and after 500 h of exposure to saline environments. Among the tested formulations, those based on TDI (L-75), that is, aromatic isocyanate, demonstrated excellent resistance to corrosion. This may be due to the increase in crystallinity and close packing of the polymer chains by stacking, which prevents the diffusion of salts. Additionally, the high concentration of polar functional groups may have enhanced the adhesion to the metal substrate, further contributing to the protective nature of the coatings.

CONCLUSIONS

This research successfully demonstrated a sustainable and scalable approach to the depolymerization of polyurethane (PU) elastomeric waste using itaconic acid without the need for glycol. The process was optimized by evaluating the effects of PU

Fig. 15 Corrosion resistance of PU coatings above (0 h) and below (500 h).

waste to acid ratios, reaction time and temperature 5:1 ratio at 165 °C for 180 min was identified as optimal conditions yielding high hydroxyl and acceptable acid and ester values. Comprehensive characterization confirmed the breakdown of the urethane linkage and formation of functional oligomers. They were effectively incorporated into the coatings and exhibited excellent gloss, hardness, flexibility and chemical resistance. TDI-based coatings showed superior anticorrosive performance, as evidenced by salt spray, Tafel polarization and impedance studies. Overall, the findings highlight the potential of this acidolysis route for converting PU elastomer waste streams into high-value polyols, supporting circular economy goals and offering promising applications in protective coatings.

Conflict of Interests

The authors declare no interest conflict.

Data Availability Statement

The related data of this paper is data that should not be shared and can be obtained from the author for reasonable reasons. The author's contact information as.sabnis@ictmumbai.edu.in.

ACKNOWLEDGMENTS

This work was financially supported by the Department of Science & Technology (DST), GOI under its INSPIRE program (No. IF240233). We are thankful to Covestro India Pvt. Ltd., Mumbai, for providing the isocyanates and Jay Elastomers Pvt., Navi Mumbai, India for providing the elastomeric waste.

REFERENCES

1 Simón, D.; Borreguero, A. M.; de Lucas, A.; Gutiérrez, C.;

Graphical Abstract

From Waste to Coatings: Acidolysis of Polyurethane Elastomers with Itaconic Acid for Polyurethane Coating

Devesh Sane, Neel Godbole, Debarati Maity, and Anagha Sabnis

Institute of Chemical Technology Nathalal Parekh Marg, India

Polyurethane elastomer waste was depolymerized using itaconic acid in a glycol-free system to obtain hydroxyl-functional oligomers. The reaction parameters governed the chemical functionalities. The recycled oligomers were directly utilized for coating formulations, demonstrating an efficient, simplified route for polyurethane (PU) waste valorization.

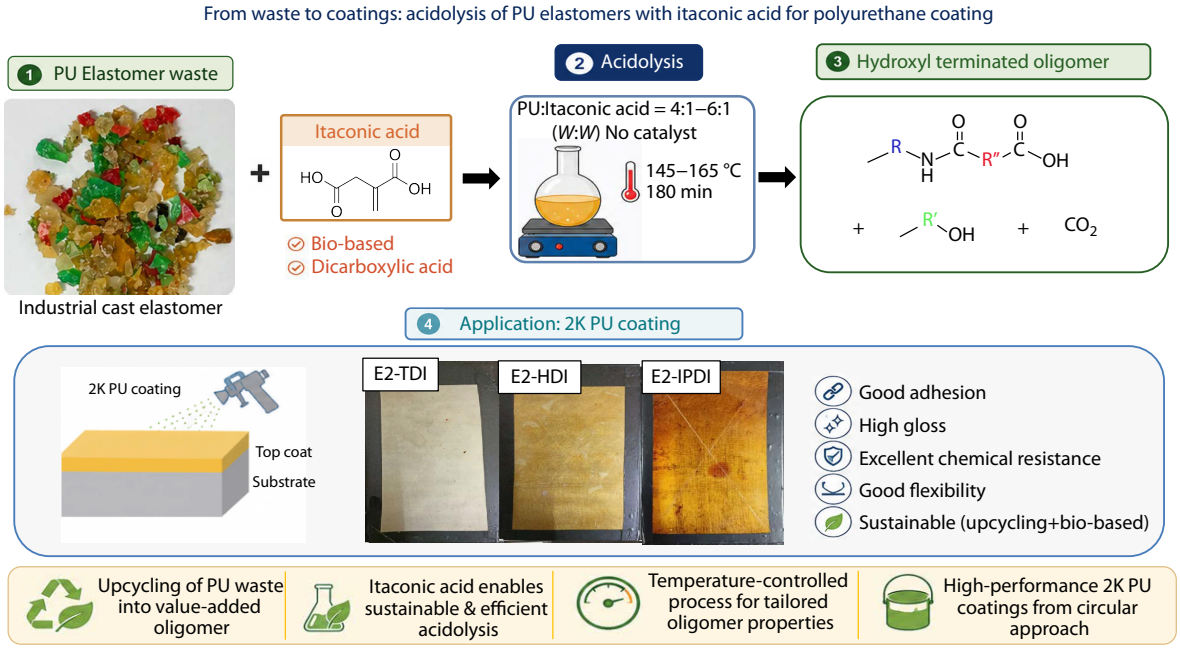

Chinese J. Polym. Sci. 2026, 44, 3340–3354 *https://doi.org/10.1007/s10118-026-3720-8*

Rodríguez, J. F. Sustainable polyurethanes: chemical recycling to get it. Environment, energy and climate change I. Cham: Springer, **2014**, pp. 229–260.

2 Sane D, Gadekar A, Jamdar V, Sabnis S. Recycling of polyurethanes. In *Polyurethanes: preparation, properties, and applications*, Volume 1: Fundamentals. ACS Symposium Series American Chemical Society, **2023,** pp. 161–179.

3 Szycher M. Szycher's handbook of polyurethanes, CRC press, **1999**, pp. 13–17.

4 Deng, Y.; Dewil, R.; Appels, L.; Ansart, R.; Baeyens, J.; Kang, Q. Reviewing the thermo-chemical recycling of waste polyurethane foam. *J. Environ. Manag.* **2021**, *278*, 111527.

5 Kiss, G.; Rusu, G.; Peter, F.; Tănase, I.; Bandur, G. Recovery of flexible polyurethane foam waste for efficient reuse in industrial formulations. *Polymers* **2020**, *12*, 1533

6 Paabo, M.; Levin, B. C. A review of the literature on the gaseous products and toxicity generated from the pyrolysis and combustion of rigid polyurethane foams. *Fire Mater.* **1987**, *11*, 1–29.

7 Gama, N.; Godinho, B.; Madureira, P.; Marques, G.; Barros-Timmons, A.; Ferreira, A. Polyurethane recycling through acidolysis: current status and prospects for the future. *J. Polym. Environ.* **2024**, *32*, 4777–4793.

8 Datta J, Włoch M. Recycling of polyurethanes. in *Polyurethane polymers*, Elsevier, **2017**, pp. 323–358.

9 Shah, H. H.; Amin, M.; Iqbal, A.; Nadeem, I.; Kalin, M.; Soomar, A. M.; Galal, A. M. A review on gasification and pyrolysis of waste plastics. *Front. Chem.* **2023**, *10*, 960894.

10 Achilias, D. S. Thermo-chemical recycling of plastics as a sustainable approach to the plastic waste issue. *Euro Mediterr. J. Environ. Integr.* **2025**, *10*, 2605–2618.

11 Guchait, A.; Maity, D.; Sabnis, A. S. Recycling of waste polyurethane shoe sole *via* aminolysis route. *J. Mater. Cycles Waste Manag.* **2024**, *26*, 860–871.

12 Nikje, M. M. A.; Garmarudi, A. B.; Idris, A. B. Polyurethane waste reduction and recycling: From bench to pilot scales. *Des. Monomers Polym.* **2011**, *14*, 395–421

13 del Amo, J.; Borreguero, A. M.; Ramos, M. J.; Rodríguez, J. F. Glycolysis of polyurethanes composites containing nanosilica. *Polymers* **2021**, *13*, 1418.

14 Zahedifar, P.; Pazdur, L.; Vande Velde, C. M. L.; Billen, P. Multistage chemical recycling of polyurethanes and dicarbamates: A glycolysis–hydrolysis demonstration. *Sustainability* **2021**, *13*, 3583

15 Brzeska, J.; Heimowska, A.; Sikorska, W.; Jasińska-Walc, L.; Kowalczuk, M.; Rutkowska, M. Chemical and enzymatic hydrolysis of polyurethane/polylactide blends. *Int. J. Polym. Sci.* **2015**, *2015*, 795985.

16 Troev, K.; Tsekova, A.; Tsevi, R. Chemical degradation of polyurethanes: degradation of flexible polyester polyurethane foam by phosphonic acid dialkyl esters. *J. Appl. Polym. Sci.* **2000**, *78*, 2565–2573

17 Soltysinski, M.; Piszczek, K.; Romecki, D.; Narozniak, S.; Tomaszewska, J.; Skorczewska, K. Conversion of polyurethane technological foam waste and post-consumer polyurethane mattresses into polyols–industrial applications. *Polimery* **2018**, *63*, 234–238.

18 Gadhave, R. V.; Srivastava, S.; Mahanwar, P. A.; Gadekar, P. T. Recycling and disposal methods for polyurethane wastes: a review. *Open J. Polym. Chem.* **2019**, *9*, 39–51.

19 Gama, N.; Godinho, B.; Marques, G.; Silva, R.; Barros-Timmons, A.; Ferreira, A. Recycling of polyurethane by acidolysis: The effect of reaction conditions on the properties of the recovered polyol. *Polymer* **2021**, *219*, 123561.

20 Godinho, B.; Gama, N.; Barros-Timmons, A.; Ferreira, A. Recycling of polyurethane wastes using different carboxylic acids *via* acidolysis to produce wood adhesives. *J. Polym. Sci.* **2021**, *59*, 697–705.

21 Gama, N.; Godinho, B.; Marques, G.; Silva, R.; Barros-Timmons, A.; Ferreira, A. Recycling of polyurethane scraps *via* acidolysis. *Chem. Eng. J.* **2020**, *395*, 125102.

22 Grdadolnik, M.; Drinčić, A.; Oreški, A.; Onder, O. C.; Utroša, P.; Pahovnik, D.; Žagar, E. Insight into chemical recycling of flexible polyurethane foams by acidolysis. *ACS Sustainable Chem. Eng.* **2022**, *10*, 1323–1332.

23 Omrani, I.; Mohammadi Berenjegani, R. Chemical recycling of flexible polyurethane foam scraps using bio-based acidolysis agents. *ACS Appl. Polym. Mater.* **2024**, *6*, 10698–10705.

24 O'Dea, R. M.; Nandi, M.; Kroll, G.; Arnold, J. R.; Korley, L. T. J.; Epps, T. H. III. Toward circular recycling of polyurethanes: Depolymerization and recovery of isocyanates. *JACS Au* **2024**, *4*, 1471–1479.

25 Liu, B.; Westman, Z.; Richardson, K.; Lim, D.; Stottlemyer, A. L.; Gillis, P.; Letko, C. S.; Hooshyar, N.; Vlcek, V.; Christopher, P.; Abu-Omar, M. M. Vapor-phase dicarboxylic acids and anhydrides drive depolymerization of polyurethanes. *ACS Macro Lett.* **2024**, *13*, 435–439.

26 Liu, B.; Westman, Z.; Richardson, K.; Lim, D.; Stottlemyer, A. L.; Farmer, T.; Gillis, P.; Hooshyar, N.; Vlcek, V.; Christopher, P.; Abu-Omar, M. M. Polyurethane foam chemical recycling: Fast acidolysis with maleic acid and full recovery of polyol. *ACS Sustainable Chem. Eng.* **2024**, *12*, 4435–4443.

27 Hudson, R. F. A simple interpretation of nucleophilic reactivity. *Chimia* **1962**, *16*, 173.

28 Okabe, M.; Lies, D.; Kanamasa, S.; Park, E. Y. Biotechnological production of itaconic acid and its biosynthesis in Aspergillus terreus. *Appl. Microbiol. Biotechnol.* **2009**, *84*, 597–606.

29 Godinho, B.; Gama, N.; Barros-Timmons, A.; Ferreira, A. Recycling of different types of polyurethane foam wastes *via* acidolysis to produce polyurethane coatings. *Sustain. Mater. Technolog.* **2021**, *29*, e00330.

30 Donadini, R.; Roso, M.; Covassin, A.; Penzo, D.; Del Bianco, G.; Romagnano, S.; Modesti, M. Closing the loop of polyurethane adhesives: Acidolysis process optimization. *Int. J. Adhes. Adhes.* **2024**, *135*, 103843.

31 He, H.; Su, H.; Yu, H.; Du, K.; Yang, F.; Zhu, Y.; Ma, M.; Shi, Y.; Zhang, X.; Chen, S.; Wang, X. Chemical recycling of waste polyurethane foams: Efficient acidolysis under the catalysis of zinc acetate. *ACS Sustainable Chem. Eng.* **2023**, *11*, 5515–5523.

32 Westman, Z.; Liu, B.; Richardson, K.; Davis, M.; Lim, D.; Stottlemyer, A. L.; Letko, C. S.; Hooshyar, N.; Vlcek, V.; Christopher, P.; Abu-Omar, M. M. Influence of carboxylic acid structure on the kinetics of polyurethane foam acidolysis to recycled polyol. *JACS Au* **2024**, *4*, 3194–3204.

33 Agnoletto, A.; Godinho, B.; Vieira, F.; Ferreira, A.; Lorenzetti, A.; Barros-Timmons, A.; Gama, N. Recycling of rigid polyurethane foams *via* acidolysis. *Prog. Rubber Plast. Recycl. Technol.* **2026**, *42*, 84–97.

34 Aksu, Y.; Haykiri-Acma, H.; Yaman, S. Recycle of flexible polyurethane foam by acidolysis and reuse of recovered polyol. *J. Polym. Environ.* **2025**, *33*, 1147–1158.

35 Zhang, X.; Pu, X.; Xia, L.; Peng, W.; Ji, Y.; Xu, J.; Wu, J.; Jiang, L.; Zhao, Q.; Fang, Z.; Xie, T. Solvent- and catalyst-free bio-conversion of waste polyurethane foams into high-performance 3D printing resin. *Natl. Sci. Rev.* **2025**, *12*, nwaf501.

36 Chattopadhyay, D. K.; Webster, D. C. Thermal stability and flame retardancy of polyurethanes. *Prog. Polym. Sci.* **2009**, *34*, 1068–1133.

37 Rogulska, M. The influence of diisocyanate structure on thermal stability of thermoplastic polyurethane elastomers based on diphenylmethane-derivative chain extender with sulfur atoms. *Materials* **2023**, *16*, 2618.

38 Hau, N. N.; Huong, D. Q. Effect of aromatic rings on mild steel corrosion inhibition ability of nitrogen heteroatom-containing compounds: Experimental and theoretical investigation. *J. Mol. Struct.* **2023**, *1277*, 134884